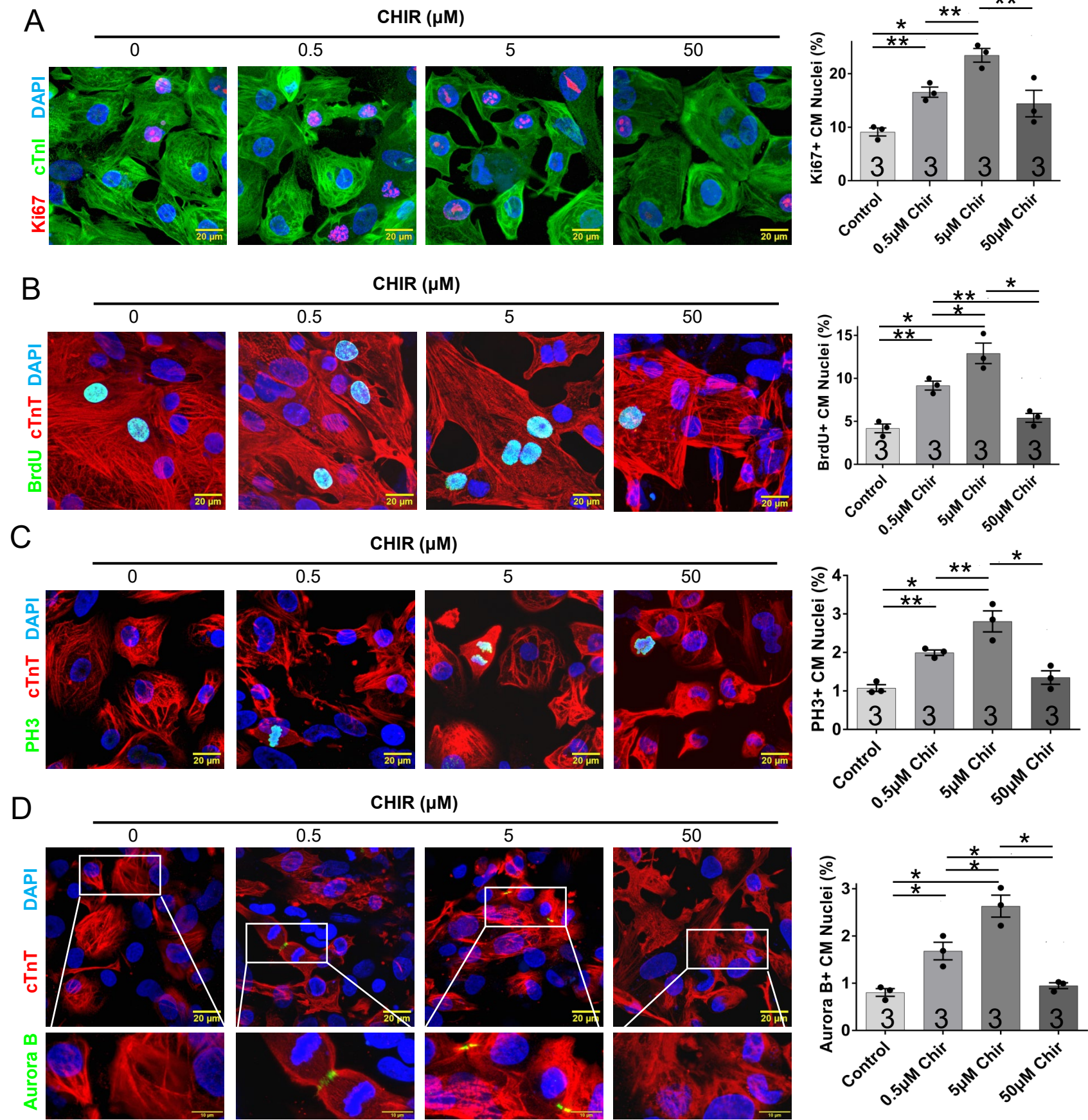
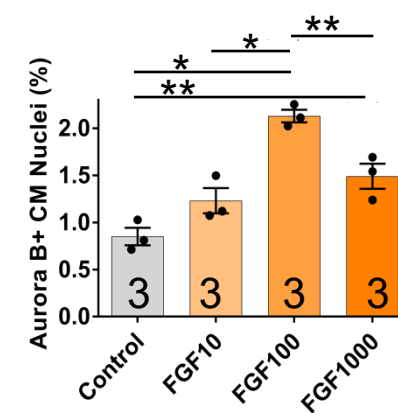
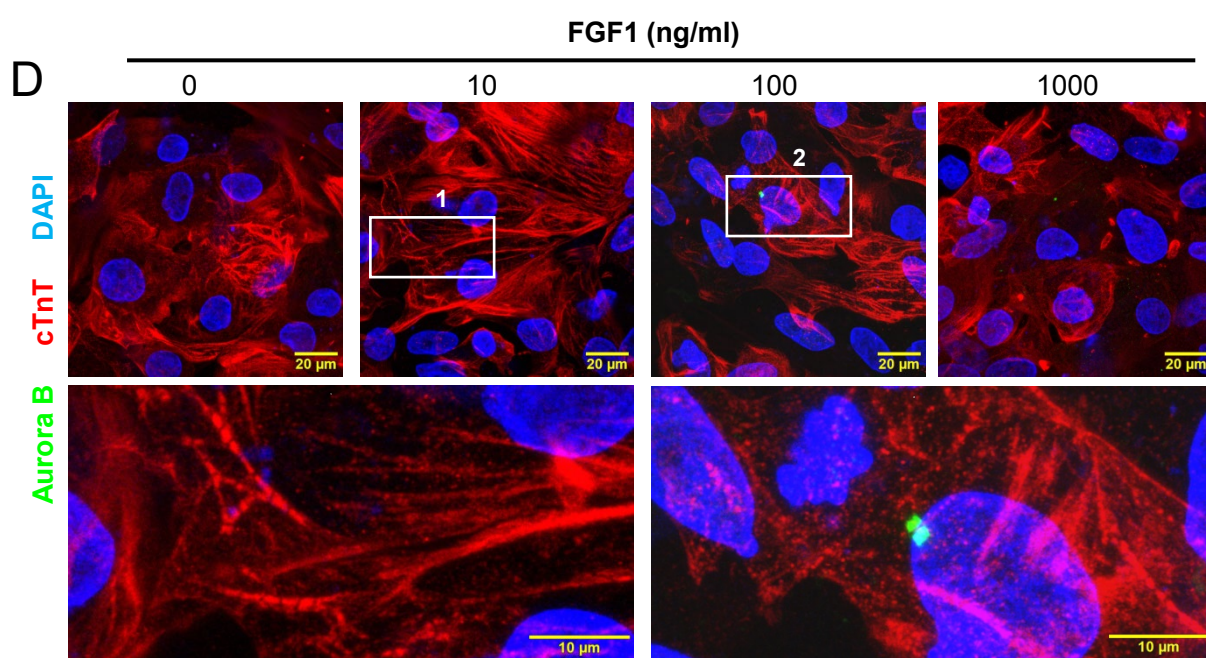
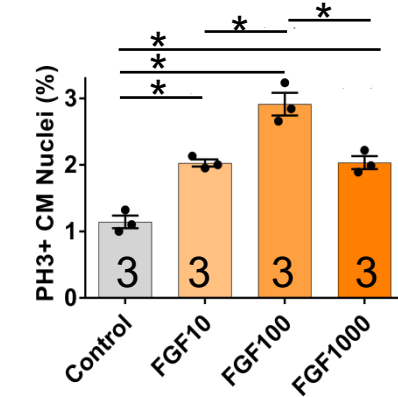
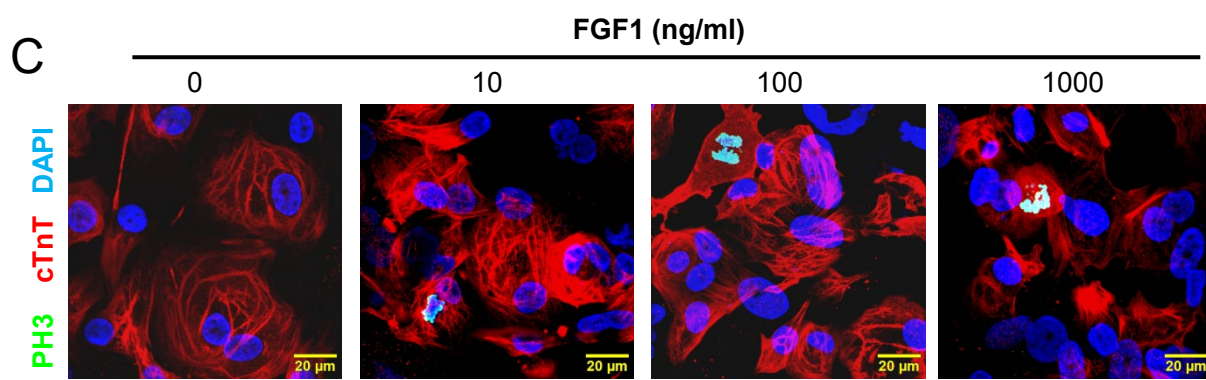
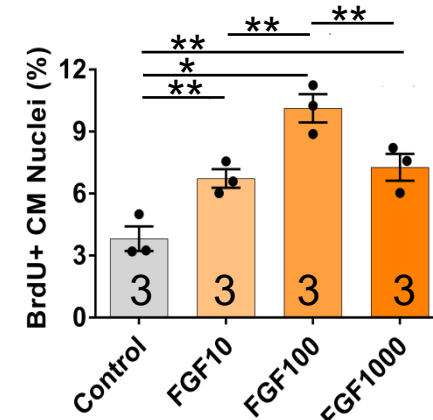
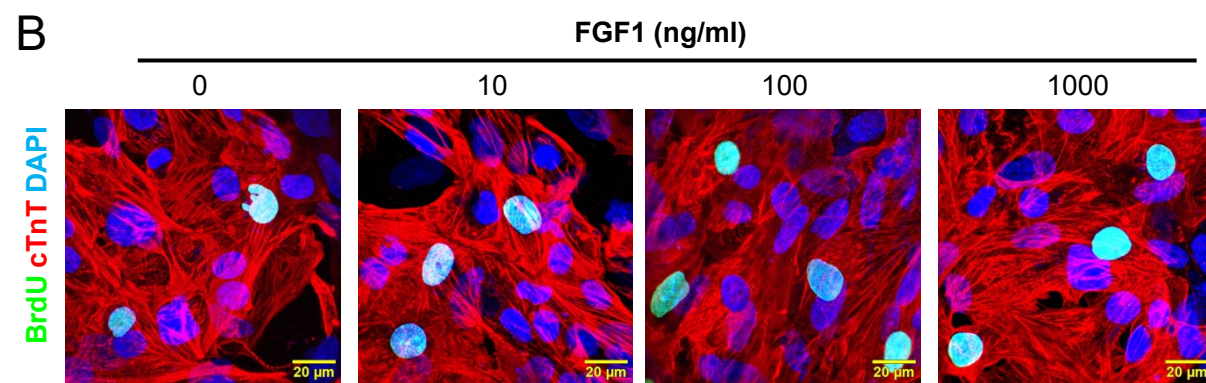
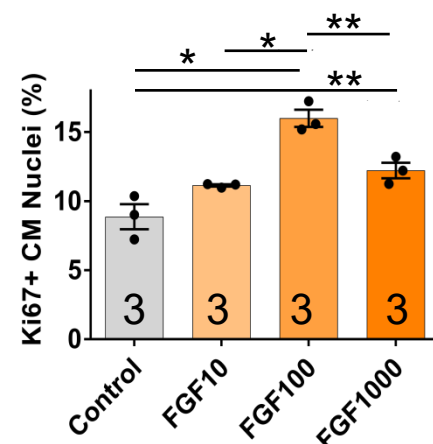
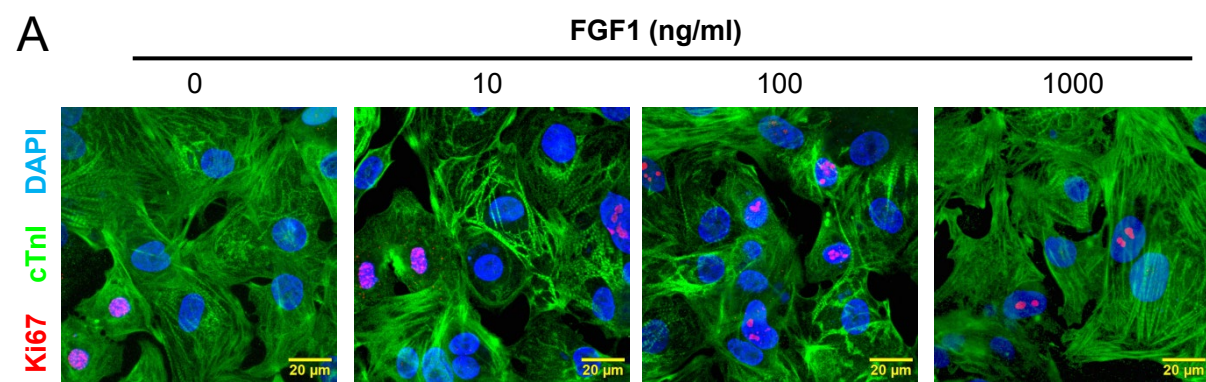


Supplemental Figure 1.

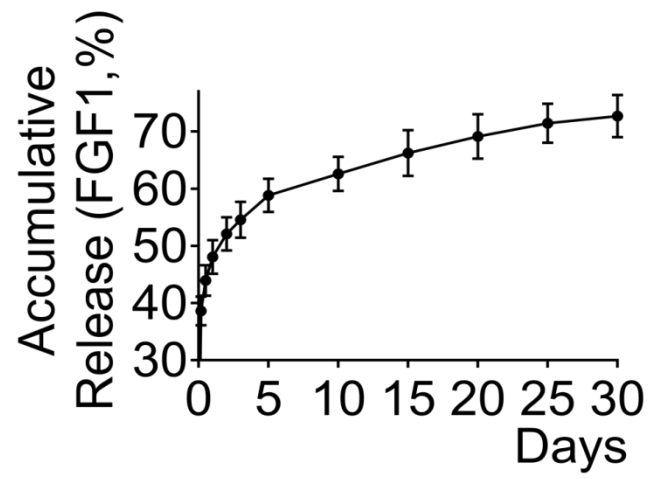
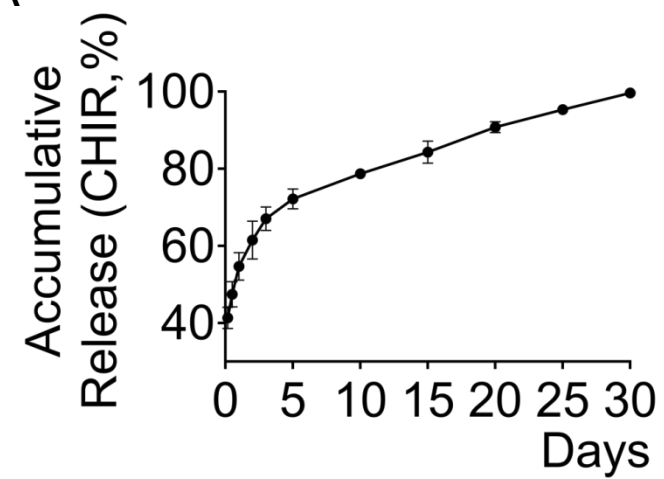


Supplemental Figure 2.



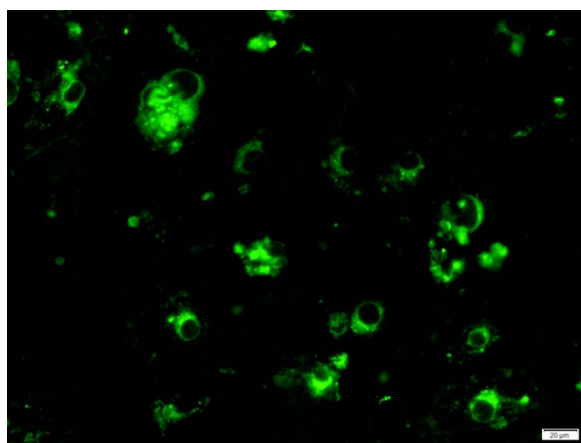
Supplemental Figure 3.

A

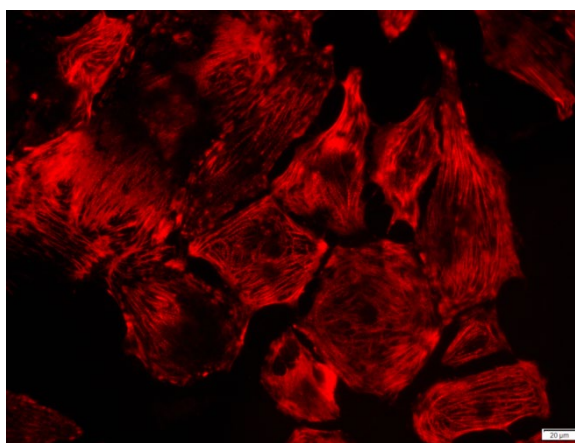


B

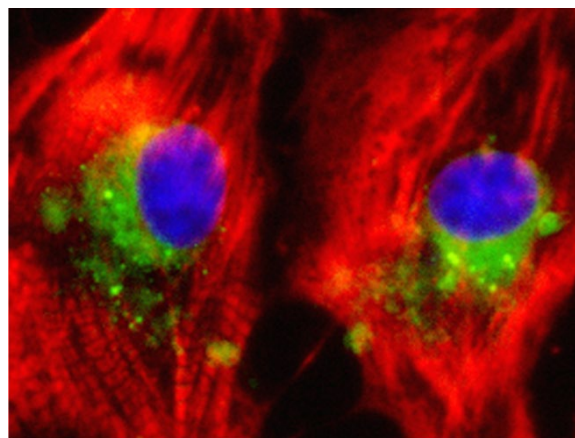
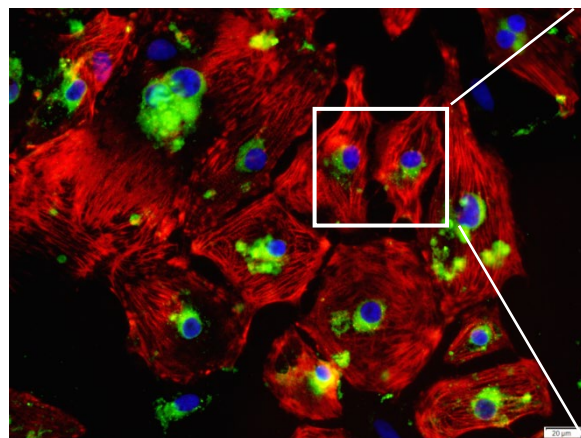
NPs



cTnT

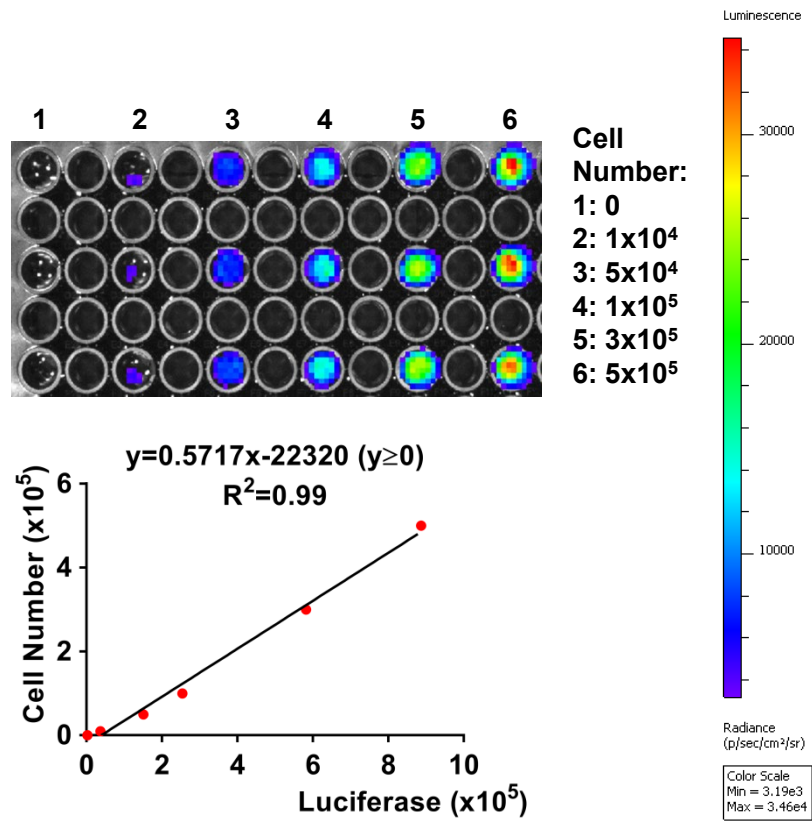


Merge (NPs cTnT DAPI)

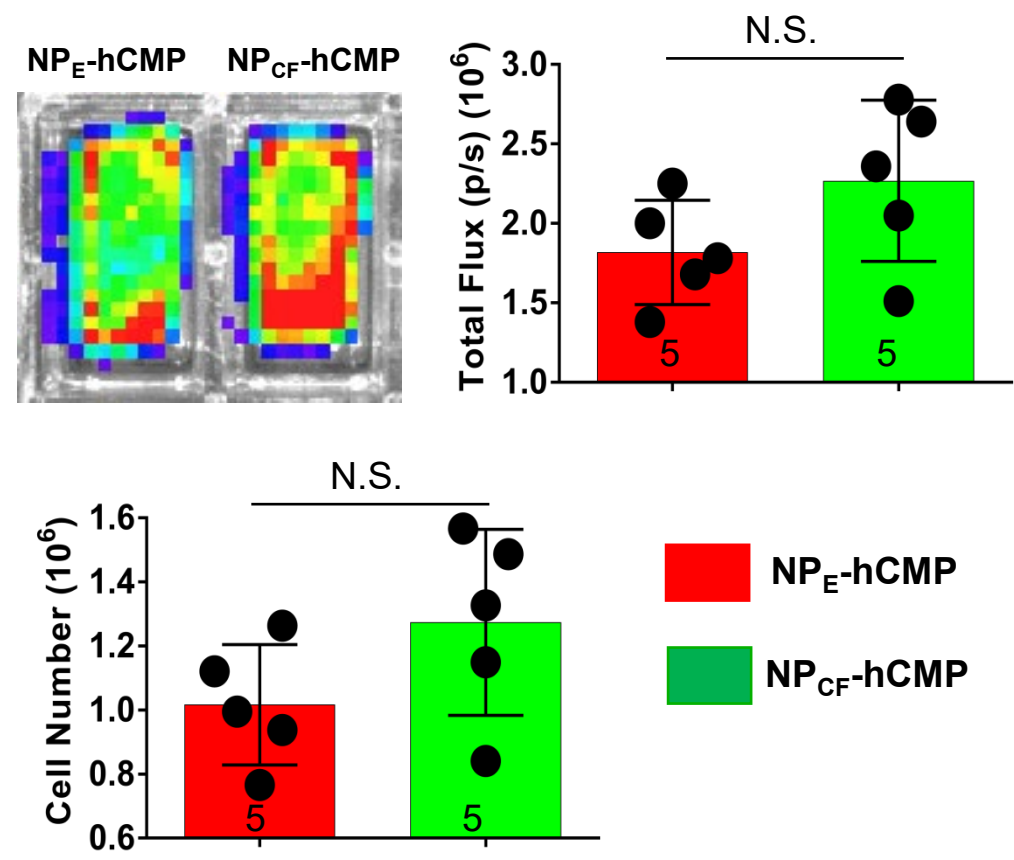


Supplemental Figure 4.

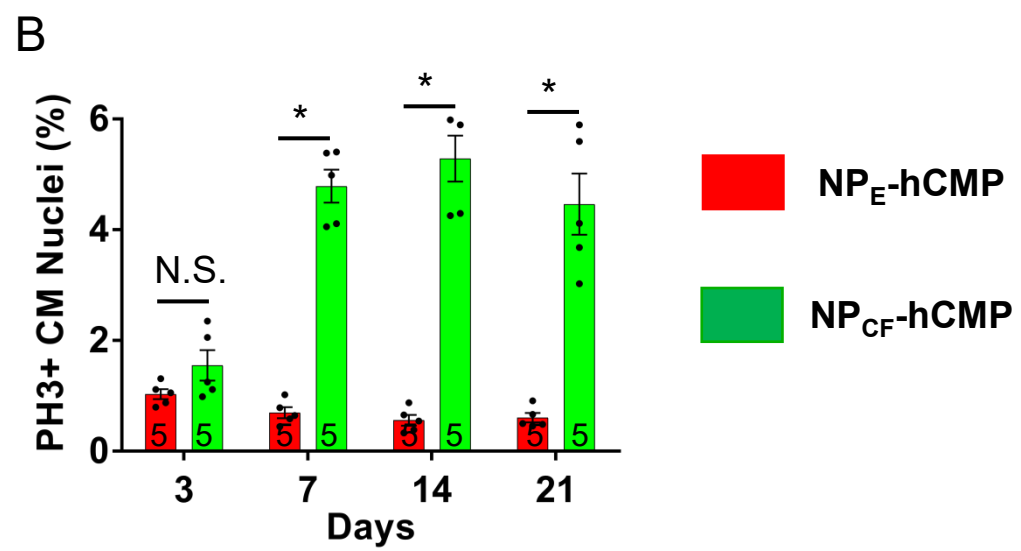
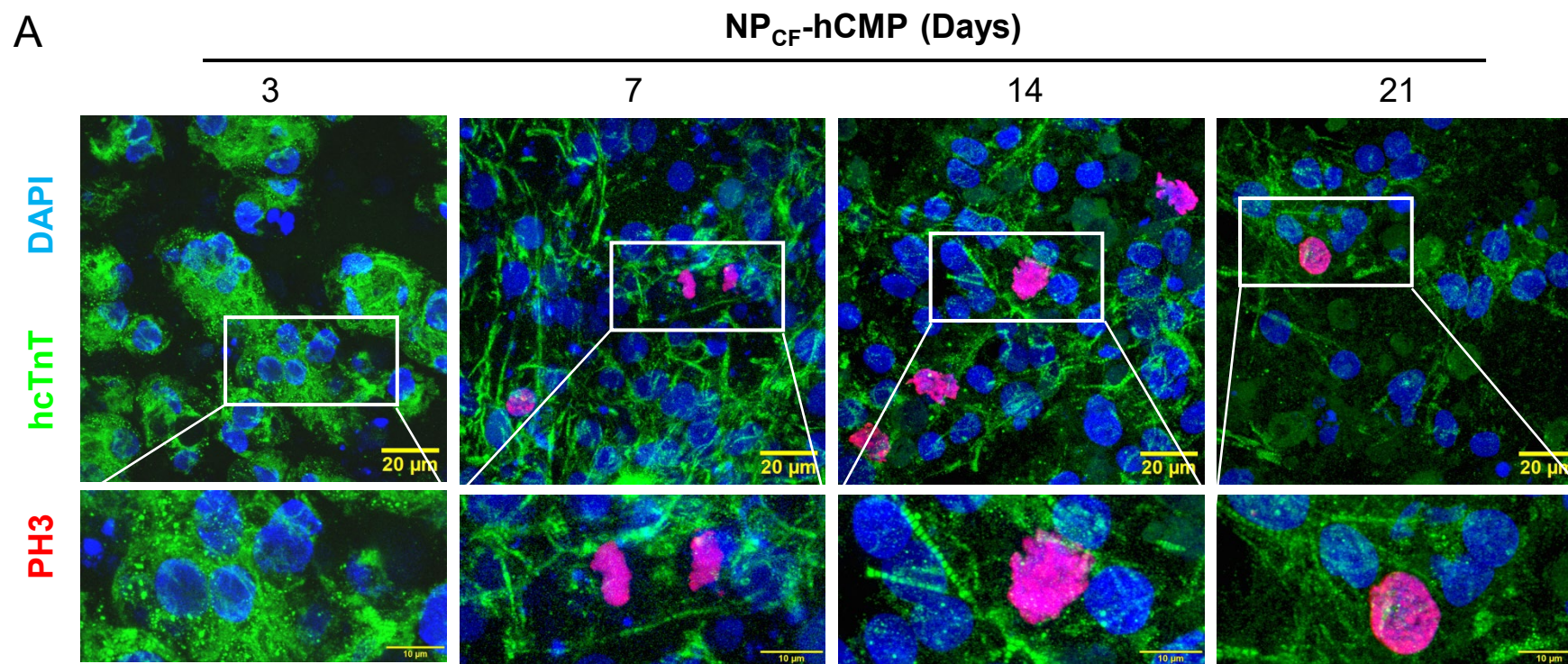
A



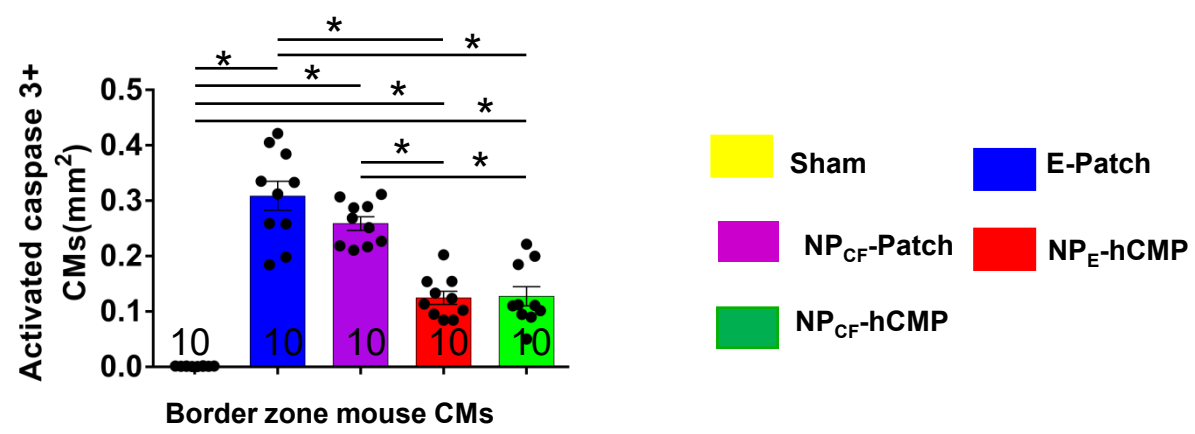
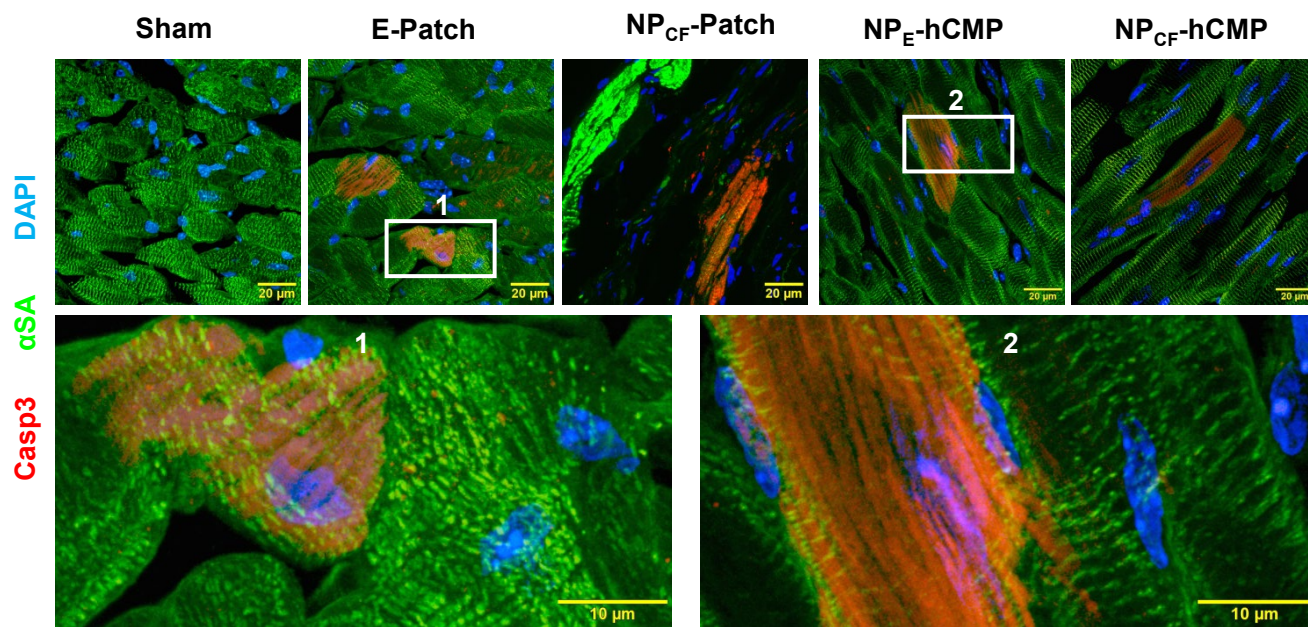
B



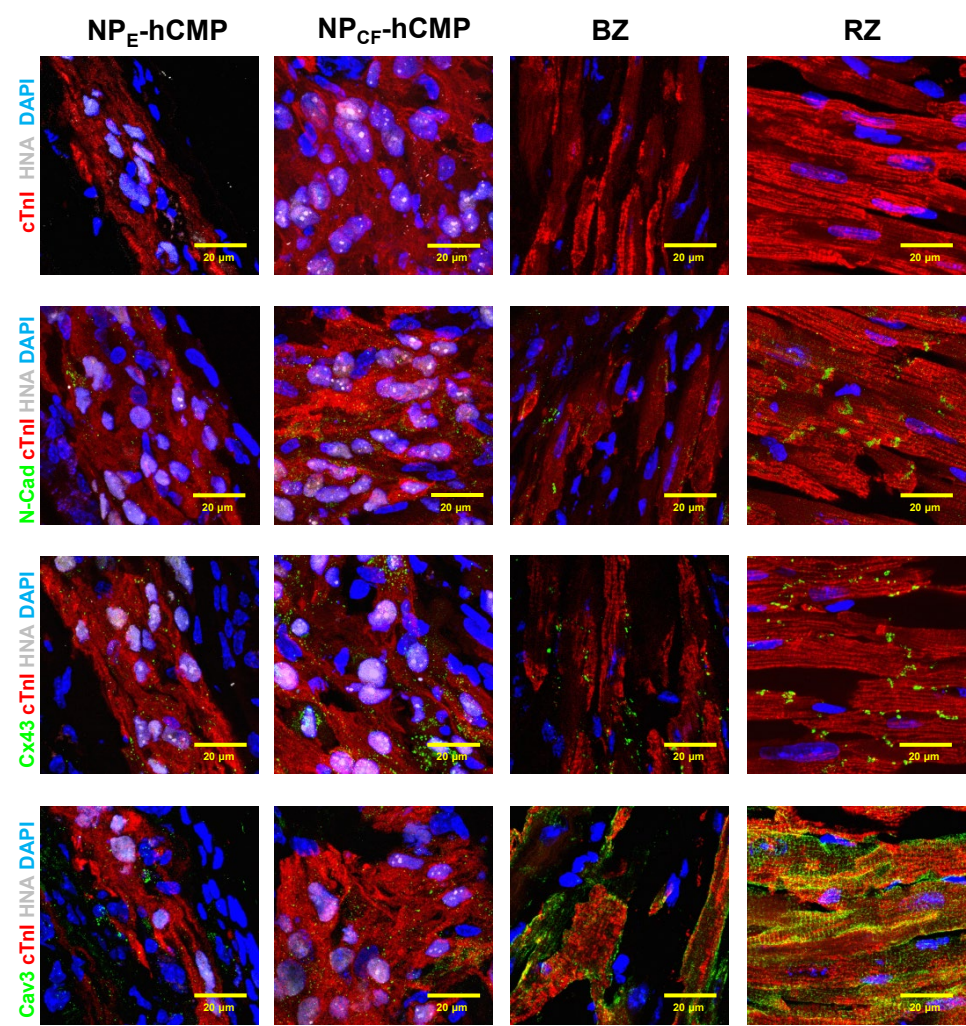
Supplemental Figure 5.



Supplemental Figure 6.



Supplemental Figure 7.



CHIR99021 and Fibroblast Growth Factor 1 Enhance the Regenerative Potency of Human Cardiac Muscle Patch after Myocardial Infarction in Mice

SUPPLEMENTAL MATERIALS

Methods

All experimental protocols were approved by The Institutional Animal Care and Use Committee (IACUC) of the University of Alabama at Birmingham and performed in accordance with the National Institutes of Health Guide for the Care and Use of Laboratory Animals (NIH publication No 85-23). All assessments were conducted by an investigator who was blinded to the experimental condition and/or treatment group. Antibodies and reagents are listed in Supplemental Tables 2 and 3.

Differentiation of human induced-pluripotent stem cells (hiPSCs) into cardiomyocytes (hiPSC-CMs).

hiPSCs were generated from cardiac fibroblasts and engineered to express a luciferin reporter gene from a ubiquitous promoter (the murine stem-cell virus promoter) as described previously [1, 2]. The hiPSCs were maintained on Matrigel Membrane Matrix (Thermo Fisher Scientific, Cat: CB356253) in mTeSR™ 1 basal and supplement medium (Stem Cell Technologies, Cat: 85850) until 75% confluent, and then differentiated into hiPSC-CMs as described previously [2, 3]. Briefly, the cells were cultured in basal medium (RPMI 1640 medium supplemented with 2% B27 supplement minus insulin; Gibco™ Cat: 11875119 and A1895601) with CHIR99021 (a GSK-3 inhibitor; Stem Cell Technologies, Cat: 72054) for 24 hours; then, the medium was replaced with CHIR99021-free basal medium. Seventy-two hours later, IWR-1 (a Wnt inhibitor; Stem Cell Technologies, Cat: 72564) was added, and the cells were cultured for 48 hours; then, the medium was replaced with RPMI 1640 medium containing 2% B27 supplement (Gibco™ Cat: 17504044). The medium was changed every 3 days afterward, and beating cardiomyocytes began to appear 9-12 days after differentiation was initiated. The hiPSC-CMs were purified by replacing the medium with glucose-free RPMI 1640 medium (Gibco™ Cat: 11879020) supplemented with 2% B27, and the medium was changed every 3 days until 4 weeks after differentiation was initiated before the patch was fabricated. The purity of the hiPSC-CM population (>95%) was evaluated via flow cytometry as described previously [2].

Generation of poly(lactic-co-glycolic acid) (PLGA) nanoparticles

PLGA nanoparticles were generated as described previously [4] and loaded with recombinant human FGF1 (rhFGF1, aa 16-155) via double-emulsion (water/oil/water phase), with CHIR99021 via single-emulsion (oil/water phase), or with Coumarin-6 via double-emulsion (water/oil/water phase). Briefly, a solution of PLGA (100 mg),

(Poly[D,L-lactide-co-glycolide]; Sigma-Aldrich Cat: 719897 for FGF1 and coumarin-6, 719900 for CHIR99021, in dichloromethane (5 mL) (Thermo Fisher Scientific, Cat: AC406910025) with or without FGF1 (200 μ L at 1 mg/mL), CHIR99021 (200 μ L at 8 mg/mL), or coumarin-6 (1 mg; Sigma-Aldrich Cat: 442631) was sonicated at 4°C for 2 minutes (40% amplitude, pulse 40 seconds, pause 20 seconds); then, 20 mL of 4% (w/v) polyvinyl alcohol (PVA) (Sigma-Aldrich Cat: 341584) solution was added for FGF1 or coumarin-6, 20 mL of 1% (w/v) dimethylamine borane (DMAB) (Sigma-Aldrich Cat: 359025) solution was added for CHIR99021. The mixtures were sonicated at 4°C for 2 minutes (40% amplitude, pulse 40 seconds, pause 20 seconds), transferred with 10 mL of 4% (w/v) PVA solution and 20 mL of Milli-Q water for FGF1 or coumarin-6, with 30 mL of Milli-Q water for CHIR99021 into a 100 mL glass beaker, and then stirred for 4 hours. After the dichloromethane evaporated completely, the solutions were spun at 1000 g for 10 minutes to remove any aggregates, and the supernatants were centrifuged again at 45000 g for 20 minutes to collect the nanoparticles. The nanoparticles were washed twice by resuspending them in 50 mL of Milli-Q water; then, the suspensions were centrifuged at 45000 g for 20 minutes, frozen at –80°C overnight, lyophilized for 48 hours, and stored at –80°C until use.

Characterization of PLGA nanoparticles

The size (diameter) of the PLGA nanoparticles was measured with a Quanta scanning electron microscope (Quanta FEG 650, Hillsboro, OR) and quantified with NIH ImageJ software. The kinetics of FGF1 and CHIR99021 release was determined by incubating the nanoparticles in phosphate-buffered saline (PBS) with 0.1% bovine serum albumin (BSA) and 0.02% sodium azide at 37°C under constant shaking, withdrawing and replacing 14.5 mL of the medium at the indicated time points, and then measuring CHIR99021 and FGF1 levels in the withdrawn medium via nanodrop (CHIR99021) or enzyme-linked immunosorbent assay (ELISA) (FGF1).

hiPSC-CM uptake of PLGA nanoparticles

hiPSC-CMs (3×10^4 cells/well) were seeded onto a Lab-Tek™ chamber slide system (Nunc™, Thermo Fisher Scientific), synchronized via serum deprivation for 24 hours, treated with coumarin-6–loaded nanoparticles (2 μ g/mL), and incubated in DMEM at 37°C under 5% CO₂. Twenty-four hours later, the cells were washed twice with PBS (pH 7.4) and viewed under a fluorescence microscope.

Fabrication of a contracting, fibrin-based, human cardiomyocyte patch (hCMP).

The fibrin-based patch was manufactured as described previously [4]. hiPSC-CMs were dispersed by incubation with Versene (Cat# 15040066, Fisher Scientific Inc) and resuspended in PBS; then, one million of the cells were added to a solution containing 0.06 mL of 25 mg/mL fibrinogen (Sigma-Aldrich Cat: F8630) and 0.28 mL of 20 mM

HEPES, and a second solution was prepared from 0.0085 mL thrombin (20 U/mL; Thermo Fisher Scientific, Cat: ICN15416301), 0.0065 mL CaCl₂ (2 M), and 0.13 mL RPMI 1640 medium with or without 15 µL of the CHIR99021- and FGF1-containing (20 µg/µL and 13.33 µg/µL, respectively) nanoparticles, as indicated. The two solutions were mixed in one well of 4-chamber culture slide to a final volume of 0.5 mL, and the mixture solidified within a few minutes to form an hCMP (dimensions: 10×17×3 mm). The patch was cultured in RPMI 1640 medium containing 20% fetal bovine serum (FBS), 1× penicillin-streptomycin, and 2 mg/mL 6-aminocaproic acid (Thermo Fisher Scientific, Cat: AC103301000) for 24 hours and then in RPMI 1640 medium containing B27, 1× penicillin-streptomycin, and 2 mg/mL 6-aminocaproic acid with daily medium changes. Isolated areas of contracting cells typically appeared three days after patch manufacture. Patches were cultured for a total of 7 days before transplantation.

Mouse myocardial infarction (MI) model and treatment

MI was surgically induced in NOD/SCID Gamma mice (stock #005557; The Jackson Laboratory). Mice were anesthetized with inhaled isoflurane (2%), intubated, and ventilated; then, a left thoracotomy was performed, and the left anterior descending coronary artery (LAD) was ligated with a 6-0 non-absorbable suture. Animals in the NP_{CF}-hCMP group were treated with hCMPs fabricated from hiPSC-CMs, CHIR99021-loaded nanoparticles, and FGF1-loaded nanoparticles, animals in the NP_E-hCMP group were treated with hCMPs composed of hiPSC-CMs and empty nanoparticles, animals in the NP_{CF}-Patch group were treated with a cell-free patch that contained only the CHIR99021- and FGF1-loaded nanoparticles, and animals in the E-Patch group were treated with patches lacking both cells and nanoparticles; a fifth group of animals (the Sham group) underwent all surgical procedures for MI induction except LAD ligation and recovered without any of the experimental treatments. The hCMPs or patches were positioned over the infarcted region of the left-ventricular (LV) anterior wall and sutured to the visceral layer of the pericardium; then, the chest muscles and skin were closed, and the animals were allowed to recover with intraperitoneal injections of buprenorphine (0.1 mg/kg) every 12 hours for up to three days and carprofen (5 mg/kg) every 12 hours for up to one day after surgery.

Engraftment rate

Because the hiPSCs carried a luciferin reporter gene and were of human origin [5], engraftment was determined both via in-vivo bioluminescence imaging (BLI) and by histological assessments of cells that co-expressed human nuclear antigen (HNA) and the human variant of cardiac troponin T (hcTnT) [2]. BLI was performed in the Small Animal Imaging Shared Facility of the University of Alabama, Birmingham, with a Xenogen IVIS-100 system. Briefly, a standard curve was generated from BLI measurements of known quantities (0, 1×10⁴, 5×10⁴, 1×10⁵, 3×10⁵, and 5×10⁵) of

hiPSC-CMs that had been digested and plated in 96-well plates; then, mice were anesthetized with isoflurane and intraperitoneally injected with D-luciferin (375 mg/kg body weight). Ten minutes later, after the luciferin had traveled to the heart and been converted to optically active oxyluciferin [6], the number of engrafted cells was determined by comparing BLI signal intensity in the front left chest region to the standard curve [5]. Histological assessments of the engraftment rate were performed as described previously [7]. Cells that expressed both hcTnT and HNA were counted in every thirtieth serial section of the whole heart (Five randomly selected and one stitched full viewing fields were evaluated per section and at least twenty sections were evaluated per animal), and the total was multiplied by 30 to obtain the number of engrafted hiPSC-CMs per heart; then, the engraftment rate was calculated by dividing the total number of engrafted hiPSC-CMs by the number used in hCMP manufacture (1×10^6) and expressed as a percentage.

Graft areas, scar areas, and LV areas

Hearts were frozen, and coronal sections were cut from the apex to the base at 10 μm intervals; Cells that expressed both hcTnT and HNA were counted in every thirtieth serial section of the whole heart (the stitched full viewing field was evaluated to measure the graft area per section and at least twenty sections were evaluated per animal), and the total was multiplied by 30 to obtain the graft area per heart; the same sections were also used to calculate the scar areas and LV areas. Scar tissue was identified with sirius red, functional myocardial tissue was identified with fast green.

Echocardiography

Echocardiography was performed as described previously [8]. Mice were lightly anesthetized with 1% inhaled isoflurane, and the heart rate was stabilized at 400-500 beats/min; then, B-mode and two-dimensional M-mode images were obtained from long-axis and short-axis views with a Vevo 2100 system (Visualsonics, Toronto, ON, Canada). Measurements were performed offline with Vevo analysis software and used to calculate the LV ejection fraction (LVEF), fractional shortening (LVFS), end-diastolic diameter (LVEDD), and end-systolic diameter (LVESD).

Infarct size and wall thickness

Infarct size was evaluated as described previously [2, 9]. Briefly, hearts were frozen, and coronal sections were cut from the apex to the base at 10 μm intervals; then, every thirtieth serial section (at least twenty sections per heart) was fixed in Bouin's solution and stained with sirius red to identify scar tissue and with fast green to identify functional myocardial tissue. Digital photographs were taken and analyzed with NIH Image-J1.36b software, and infarct size was calculated according to the following formula: Infarct size = (scar surface area)/(total LV surface area) \times 100%. LV anterior wall thickness was

obtained from the same sections and staining; five randomly selected viewing fields per section and at least twenty sections per heart were measured.

Cell cycle activity and proliferation

Cell cycle activity and proliferation were evaluated in both cultured hiPSC-CMs and cryopreserved heart sections [3, 9, 10] via immunofluorescence analyses of 5-bromo-2'-deoxy-uridine (BrdU) incorporation and of the expression of Ki67, phosphorylated histone 3 (PH3), and Aurora B. For cultured hiPSC-CMs, cell cycles were synchronized via serum deprivation, and then the cells were plated onto a 6-well dish in RPMI 1640 medium supplemented with 2% B27 and maintained for 4 weeks; then, the cells were rinsed twice with PBS (pH 7.4) and incubated with serum-free Dulbecco's Modified Eagle's Medium (DMEM) containing 4.5 g/L glucose, L-glutamine, and sodium pyruvate (Corning Cat: MT10013CV). Twenty-four hours later, the cells were treated with or without CHIR99021 (0.5 μ M, 5 μ M, 50 μ M), FGF1 (10 ng/mL, 100 ng/mL, or 1000 ng/mL; R&D Systems™ Cat: 232-FA), or both CHIR99021 (5 μ M) and FGF1 (100 ng/mL) for 24 hours.

In-vitro BrdU labeling was performed by incubating the hiPSC-CMs with BrdU (10 μ mol) in a humidified atmosphere under 5% CO₂ at 37°C for 12 hours. In-vivo BrdU labeling was performed by intraperitoneally injecting mice with BrdU (0.2 mg per gram of body weight per day) for 2 consecutive days before sacrifice; then, hearts were harvested, frozen, and cut into 10- μ m thick sections, and the sections were fixed with the ethanol fixative according to the manufacturer's instructions (Cat# 11296736001, Roche). The BrdU labeling was detected in both cells and tissue sections by using a BrdU Labeling and Detection Kit (Roche) as directed by the manufacturer's instructions, and the expression of Ki67, PH3, and Aurora B was detected with the corresponding antibodies.

Apoptosis

Apoptosis was evaluated in both cultured hiPSC-CMs and cryopreserved heart sections [3, 9, 11]. Cultured hiPSC-CMs were treated with or without CHIR99021 (5 μ M), FGF1 (100 ng/mL), or both CHIR99021 and FGF1 for 2 hours, placed in an incubator, and cultured under 1% O₂, 5% CO₂, and 94% N₂ for 24 hours; then, the cells were washed and fixed with 4% paraformaldehyde for 30 minutes. Apoptosis was analyzed via TUNEL assay with an In Situ Cell death detection Kit (TMR red) as directed by the manufacturer's instructions (Cat# 12156792910, Millipore Sigma). Briefly, cells or tissue sections were washed in PBS, incubated with 75 μ L of equilibration buffer for 5 minutes at room temperature, incubated with 55 μ L of TdT enzyme for 1 hour at 37°C, washed with stop buffer for 10 minutes, rinsed 3 times with saline, incubated with anti-digoxigenin conjugate for 30 minutes at room temperature, and rinsed with PBS; then, slides were mounted with medium containing DAPI (Vector Laboratories, Inc. Cat# H-1200) and

viewed under a fluorescence microscope. Experiments with cultured cells were conducted in triplicate, and at least ten sections from the border zone (BZ) of the infarct were evaluated for each heart.

Immunostaining and Fluorescence Microscopy

The explanted hearts were collected at day 28 and fixed in ice-cold 4% paraformaldehyde (PFA) for 4 hours followed by overnight immersion in 30% sucrose, at 4°C. 10µm serial cryosections were generated, and every 30th section was permeabilized with 0.2% Triton X-100, for 10 minutes at room temperature. Next, sections were blocked in 5% donkey serum in DPBS, pH 7.4 for 30 minutes at room temperature. The primary antibodies used are shown in Supplemental Table 2. Primary antibodies (for apoptosis: activated caspase 3 and αSA; cardiomyocyte hypertrophy: cTnI and WGA; hiPSC-CM maturation: HNA, cTnI, N-Cad, Cx43 and Cav3) were used at 1:10 to 1:10000 dilutions in blocking buffer (1.5% BSA, 100 mM glycine in PBS) for 12 to 16 hours at 4°C. Secondary antibodies (FITC, CYTM3, and CYTM5 obtained from Jackson ImmunoResearch Laboratory) were used at 1:200 dilutions in blocking buffer for 2 hours at room temperature in the dark. Nuclei were stained with 4,6-diamidino-2-phenyl-indole (DAPI, 100 ng/ml; Sigma-Aldrich). Negative controls for staining included only secondary antibodies. Finally, the sections were analyzed using a fluorescence microscope (Olympus IX81). Five randomly selected viewing fields per section and at least ten sections from the border zone (BZ) of the infarct were evaluated for each heart.

Vascular density

Vascular density was evaluated in cryopreserved sections as described previously [3, 9, 11]. Briefly, sections were immunofluorescently stained for expression of the endothelial marker isolectin B4, and vascular density was quantified as the number of positively stained vessel-like structures per unit area.

Statistics

The data were presented as mean ± standard error of the mean (mean±SEM). Differences between two groups were evaluated for significance via the Student's t-test, and differences among three groups were evaluated for significance via analysis of variance (ANOVA). A p value < 0.05 was considered statistically significant.

References

- [1] L. Zhang, J. Guo, P. Zhang, Q. Xiong, S.C. Wu, L. Xia, S.S. Roy, J. Tolar, T.D. O'Connell, M. Kyba, K. Liao, J. Zhang, Derivation and high engraftment of patient-specific cardiomyocyte sheet using induced pluripotent stem cells generated from adult cardiac fibroblast, *Circ Heart Fail* 8(1) (2015) 156-66.
- [2] W. Zhu, M. Zhao, S. Mattapally, S. Chen, J. Zhang, CCND2 Overexpression Enhances the Regenerative Potency of Human Induced Pluripotent Stem Cell-Derived Cardiomyocytes: Remuscularization of Injured Ventricle, *Circ Res* 122(1) (2018) 88-96.
- [3] L. Gao, M.E. Kupfer, J.P. Jung, L. Yang, P. Zhang, Y. Da Sie, Q. Tran, V. Ajeti, B.T. Freeman, V.G. Fast, P.J. Campagnola, B.M. Ogle, J. Zhang, Myocardial Tissue Engineering With Cells Derived From Human-Induced Pluripotent Stem Cells and a Native-Like, High-Resolution, 3-Dimensionally Printed Scaffold, *Circ Res* 120(8) (2017) 1318-1325.
- [4] L. Gao, Z.R. Gregorich, W. Zhu, S. Mattapally, Y. Oduk, X. Lou, R. Kannappan, A.V. Borovjagin, G.P. Walcott, A.E. Pollard, V.G. Fast, X. Hu, S.G. Lloyd, Y. Ge, J. Zhang, Large Cardiac Muscle Patches Engineered From Human Induced-Pluripotent Stem Cell-Derived Cardiac Cells Improve Recovery From Myocardial Infarction in Swine, *Circulation* 137(16) (2018) 1712-1730.
- [5] S.G. Ong, B.C. Huber, W.H. Lee, K. Kodo, A.D. Ebert, Y. Ma, P.K. Nguyen, S. Diecke, W.Y. Chen, J.C. Wu, Microfluidic Single-Cell Analysis of Transplanted Human Induced Pluripotent Stem Cell-Derived Cardiomyocytes After Acute Myocardial Infarction, *Circulation* 132(8) (2015) 762-771.
- [6] N. Sun, A. Lee, J.C. Wu, Long term non-invasive imaging of embryonic stem cells using reporter genes, *Nat Protoc* 4(8) (2009) 1192-201.
- [7] Y. Nakamura, X. Wang, C. Xu, A. Asakura, M. Yoshiyama, A.H. From, J. Zhang, Xenotransplantation of long-term-cultured swine bone marrow-derived mesenchymal stem cells, *Stem Cells* 25(3) (2007) 612-20.
- [8] Q. Xiong, L. Ye, P. Zhang, M. Lepley, J. Tian, J. Li, L. Zhang, C. Swingen, J.T. Vaughan, D.S. Kaufman, J. Zhang, Functional consequences of human induced pluripotent stem cell therapy: myocardial ATP turnover rate in the in vivo swine heart with postinfarction remodeling, *Circulation* 127(9) (2013) 997-1008.
- [9] W. Zhu, W. Zhang, W. Shou, L.J. Field, P53 inhibition exacerbates late-stage anthracycline cardiotoxicity, *Cardiovasc Res* 103(1) (2014) 81-9.
- [10] W. Zhu, M.H. Soonpaa, H. Chen, W. Shen, R.M. Payne, E.A. Liechty, R.L. Caldwell, W. Shou, L.J. Field, Acute doxorubicin cardiotoxicity is associated with p53-induced inhibition of the mammalian target of rapamycin pathway, *Circulation* 119(1) (2009) 99-106.
- [11] W. Zhu, R.J. Hassink, M. Rubart, L.J. Field, Cell-cycle-based strategies to drive myocardial repair, *Pediatr Cardiol* 30(5) (2009) 710-5.

SUPPLEMENTAL TABLE 1. Release kinetics of CHIR99021 and FGF1 (%) from nanoparticles

Time (day)	0.167	0.5	1	2	3	5	10	15	20	25	30
CHIR (%)	41.36±4.72	47.44±5.67	54.69±6.14	61.5±8.52	67.05±5.26	72.2±4.47	78.76±1.74	84.34±4.99	90.82±2.48	95.39±0.54	99.68±0.37
FGF1 (%)	38.63±2.51	43.95±2.69	48.09±2.96	52.12±2.92	54.56±3.14	58.87±2.92	62.62±2.98	66.27±4.02	69.15±3.88	71.45±3.39	72.71±3.70

SUPPLEMENTAL TABLE 2. Primary antibodies

Primary antibodies	Dilutions	Source	Cat. No.
Cardiac myocyte markers			
Cardiac Troponin T	1:100	Abcam	ab188877
Sarcomeric Alpha Actinin	1:100	Abcam	ab9465
Cardiac Troponin I	1:100	Abcam	ab188877
Human NKX2.5	1:100	R&D Systems	AF2444
wheat germ agglutinin (WGA)	1:1000	Thermo Fisher Scientific	W11261
Endothelial cell markers			
Isolectin B4	1:100	Vector	FL-1201
Cell cycle markers			
Histone H3 (phospho S10)	1:100	Abcam	ab14955
Phosphorylated Histone H3	1:200	EMD Millipore	06-570
Ki-67	1:100	EMD Millipore	AB9260
Aurora B	1:100	Abcam	ab3609
BrdU	1:10	Roche	11296736001
Human cell markers			
Human Specific Cardiac Troponin T	1:100	Abcam	ab91605
Human Nucleolin Antigen	1:300	Abcam	ab198580
Cardiomyocyte Maturation Markers			
Connexin 43	1:100	Sigma-Aldrich	MABT901
N-cadherin	1:100	Sigma-Aldrich	C3865
Caveolin 3	1:100	Abcam	ab2912

SUPPLEMENTAL TABLE 3. Chemicals and medium

Chemicals	Source	Cat. No.
Matrigel	Thermo Fisher Scientific	CB356253
mTeSR™	Stem Cell Technologies	85850
RPMI 1640	Gibco	11875119
RPMI 1640 with no glucose	Gibco	11879020
B27 supplement	Gibco	17504044
B27 supplement minus insulin	Gibco	A1895601
CHIR99021	Stem Cell Technologies	72054
FGF1	R&D Systems	232-FA
IWR-1	Stem Cell Technologies	72564
DMEM	Corning	MT10013CV
PLGA for FGF1	Sigma-Aldrich	719897
PLGA for CHIR99021	Sigma-Aldrich	719900
Dichloromethane	Thermo Fisher Scientific	AC406910025
CHIR99021	Stem Cell Technologies	72054
FGF1	R&D Systems	232-FA
IWR-1	Stem Cell Technologies	72564
DMEM	Corning	MT10013CV
PLGA for FGF1	Sigma-Aldrich	719897
PLGA for CHIR99021	Sigma-Aldrich	719900
Dichloromethane	Thermo Fisher Scientific	AC406910025
Coumarin-6	Sigma-Aldrich	442631
Polyvinyl alcohol	Sigma-Aldrich	341584
Dimethylamine borane	Sigma-Aldrich	359025
Fibrinogen	Sigma-Aldrich	F8630
Thrombin	Thermo Fisher Scientific	ICN15416301
6-aminocaproic acid	Thermo Fisher Scientific	AC103301000

SUPPLEMENTAL FIGURE LEGENDS

Supplemental Fig. 1: Cell cycle activity of hiPSC-CMs treated with various concentrations of CHIR99021. The cell cycles of hiPSC-CMs were synchronized via serum starvation; then, the cells were treated with varying concentrations of CHIR99021 (0.5 μ M, 5 μ M, or 50 μ M) for 24 hours and immunofluorescently stained for the presence of cTnI or cTnT; nuclei were identified via DAPI staining. **(A)** Proliferation was evaluated via immunofluorescence analyses of Ki67 expression and quantified as the percentage of positively stained cells. **(B)** hiPSC-CMs in the S-phase of the cell cycle were identified via immunofluorescence analyses of BrdU expression and quantified as the percentage of positively stained cells. **(C)** hiPSC-CMs in the M-phase of the cell cycle were identified via analyses of PH3 expression and quantified as the percentage of positively stained cells. **(D)** hiPSC-CMs undergoing cytokinesis were identified via Aurora B expression and quantified as the percentage of positively stained cells. For each treatment group, the number of independent experiments with new cell cultures is displayed at the base of the corresponding column. Five randomly selected viewing fields were evaluated per group per experiment. * p <0.01, ** p <0.05; one-way ANOVA with Tukey correction for multiple comparisons.

Supplemental Fig. 2: Cell cycle activity of hiPSC-CMs treated with various concentrations of FGF1. The cell cycles of hiPSC-CMs were synchronized via serum starvation; then, the cells were treated with varying concentrations of FGF1 (10 ng/mL, 100 ng/mL, or 1000 ng/mL) for 24 hours and immunofluorescently stained for the presence of cTnI or cTnT; nuclei were identified via DAPI staining. **(A)** Proliferation was evaluated via immunofluorescence analyses of Ki67 expression and quantified as the percentage of positively stained cells. **(B)** hiPSC-CMs in the S-phase of the cell cycle were identified via immunofluorescence analyses of BrdU expression and quantified as the percentage of positively stained cells. **(C)** hiPSC-CMs in the M-phase of the cell cycle were identified via analyses of PH3 expression and quantified as the percentage of positively stained cells. **(D)** hiPSC-CMs undergoing cytokinesis were identified via Aurora B expression and quantified as the percentage of positively stained cells. For each treatment group, the number of independent experiments with new cell cultures is displayed at the base of the corresponding column. Five randomly selected viewing fields were evaluated per group per experiment. * p <0.01, ** p <0.05; one-way ANOVA with Tukey correction for multiple comparisons.

Supplemental Fig. 3: Release kinetics of CHIR99021 and FGF1 and the uptake of PLGA nanoparticles by hiPSC-CMs. **(A)** Release curve for CHIR99021 and FGF1 from PLGA nanoparticles. **(B)** The cell cycles of hiPSC-CMs were synchronized via serum starvation; then, the cells were treated with DMEM containing nanoparticles (2 μ g/mL) that had been loaded with coumarin-6 (green). Twenty-four hours later, the cells were washed twice with PBS and immunofluorescently stained for cTnT (red). Nuclei were counterstained with DAPI (blue), and the cells were observed with a

fluorescence microscope to confirm that they had taken-up the nanoparticles. Bar = 20 μ m.

Supplemental Fig. 4: Bioluminescence signals from hiPSC-CMs. Because the hiPSC-CMs carried a luciferase reporter, engraftment could be evaluated via bioluminescence imaging (BLI). (A) BLI signal intensities from varying known quantities of hiPSC-CMs (top) were used to generate a standard curve (bottom), which was subsequently used to calculate hiPSC-CM engraftment rates from BLI measurements in living mice. (B) Bioluminescence imaging (BLI) images of NPE-hCMPs and NPCF-hCMPs were taken 7 days after fabrication. The signal intensity was quantified and expressed as total flux. The total number of cells was calculated by comparing the signal intensity to the standard curve.

Supplemental Fig. 5: Treatment with CHIR99021 and FGF1 stimulates the cell cycle of hiPSC-CMs in cultured hCMPs. (A) Cultured NP_{CF}-hCMPs and NP_E-hCMPs were collected at the indicated time points after manufacture and immunofluorescently stained for the expression of hcTnT and the M-phase cell cycle marker PH3; nuclei were counterstained with DAPI. (B) Cell cycle activity was quantified as the proportion of hcTnT-positive cells that also expressed PH3 and present as a percentage. The number of NP_{CF}-hCMPs and NP_E-hCMPs evaluated at each time point is displayed at the base of the corresponding column. Five randomly selected viewing fields were evaluated per animal. * $p < 0.01$; two-way ANOVA with Sidak correction for multiple comparisons.

Supplemental Fig. 6: hCMP transplantation reduced caspase 3 activation after MI injury in mice. Twenty-eight days after MI induction or sham surgery, sections were collected from the BZ of the infarct in E-Patch, NP_{CF}-Patch, NP_E-hCMP, and NP_{CF}-hCMP animals, and from the corresponding region of the hearts of Sham animals, and then immunofluorescently stained for expression of the cardiomyocyte protein α sarcomeric actinin (α SA) and for the pro-apoptosis protein caspase 3 (Casp3); nuclei were counterstained with DAPI. Cardiomyocyte apoptosis was quantified as the proportion of α SA-positive cells that were also positive for caspase 3 and expressed as a percentage. The number of animals evaluated for each treatment group is displayed at the base of the corresponding column. Five randomly selected viewing fields were evaluated per section and ten sections were evaluated per animal. * $p < 0.01$, ** $p < 0.05$; one-way ANOVA with Tukey correction for multiple comparisons.

Supplemental Fig. 7: Maturation of the hiPSC-CMs in transplanted hCMPs. Twenty-eight days after MI induction, sections were collected from the region of patch administration in NP_E-hCMP-treated (first column) and NP_{CF}-hCMP-treated (second column) hearts, from the NP_E-Patch-treated border zone of the infarct (BZ, third column), and from the NP_E-Patch-treated remote (noninfarcted) zone (RZ, fourth column) and then stained for the expression of HNA to identify the engrafted human-lineage cells, and for the expression of cTnI, cTnI and N-Cadherin (N-Cad), cTnI and Connexin 43

(Cx43), and cTnI and Calveolin-3 (Cav-3); nuclei were counterstained with DAPI.